AIAA JOURNAL
Vol. 33, No. 5, May 1995

Free Vortex Calculations Using Analytical/Numerical Matching with Solution Pyramiding

Ronald J. Epstein* and Donald B. Bliss†
Duke University, Durham, North Carolina 27708

The motion of a free vortex system is predicted using a novel method called analytical/numerical matching (ANM). Analytical/numerical matching is a hybrid mathematical and numerical technique that results in a new problem formulation with high accuracy and increased computational efficiency. The approach capitalizes on the disparity of characteristic length scales that occur in many fluid dynamics problems. Accordingly, many problems can be decomposed into two distinct problems involving a local high-resolution near field, often solvable analytically, and a global, low-resolution far field, solved numerically. The ANM technique breaks the free vortex problem into these local and global problems each of which are easier and more efficient to solve than the traditional problem formulation. In addition, the ANM decomposition can be repeated to form a hierarchy of nested problems of increasing resolution using a method called pyramiding. The ANM method with pyramiding, called ANM/P, is studied to assess its accuracy and computational efficiency for two-dimensional and three-dimensional vortex dynamics problems. In calculations of vortex sheet rollup and vortex ring motion and interactions, this method was found to be relatively easy to implement and exhibited reductions in computational time from a factor of three to more than an order of magnitude.

Nomenclature

C_P	= ANM/P pyramiding constant
dA	= differential area
$d\boldsymbol{s}$	= differential displacement vector
f_c, R_f	= vortex fat core
L	= length
$\boldsymbol{l}_{si}$	= incremental vector distance
M_l	= midfield local computational domain size
m_c	= vortex midcore
N	= number of computational elements
N_c	= number of centroids
N_l	= near-field local computational domain size
$\boldsymbol{P}$	= point of evaluation
P	= number of pyramid levels
r	= magnitude of a radial position vector
$\boldsymbol{r}$	= radial position vector
r_c	= vortex core radius
$\boldsymbol{r}_{v_i}$	= incremental radial position vector distance
t_c, R_t	= vortex thin core
u, v, z	= Cartesian velocity components
$\boldsymbol{v}$	= induced velocity vector
v_θ	= rotational velocity
X_n, Y_n	= centroid position
α	= overlap constant
β	= overlap constant
Γ	= circulation around a vortex, positive or negative
γ	= variable parametric coordinate
ε	= generalized vortex core
κ	= ANM/P dispersion constant
$\zeta_{t,m,f}$	= ratio of rotational core size/computational element spacing
φ	= rotational angle in polar or cylindrical coordinates
ω	= vorticity, curl of the velocity vector

Received Nov. 18, 1993; revision received July 19, 1994; accepted for publication Aug. 1, 1994.

*Research Assistant, Department of Mechanical Engineering and Materials Science. Student Member AIAA.

†Associate Professor, Department of Mechanical Engineering and Materials Science. Member AIAA.

I. Introduction

A. Overview

MANY problems in fluid mechanics are limited by constraints on accuracy and computational efficiency. The free motion of vorticity fields tracked by Lagrangian methods is an example of a computationally intensive procedure, an important practical case being rotorcraft free wake analysis. The present paper presents a different approach to this problem using a new method called analytical/numerical matching (ANM). ANM has been used previously for vortex filament dynamics,[1,2] where the method was applied along single filaments. The present approach demonstrates how ANM can be applied to vorticity distributions, to calculate the resultant velocity or pressure fields.

The interesting feature of the ANM methodology is that it obtains accurate solutions in an efficient manner by utilizing a low-resolution solution with an analytical correction. A global numerical solution is constructed from a field of low-density, smoothed singularities. The result is corrected using an analytical local solution that removes smoothing effects and restores the high resolution associated with local structure. The basic method is explained in detail in the next section.

This paper further demonstrates that the ANM method can be applied repeatedly to a given vorticity field to produce a nested hierarchy of problems at different levels of resolution. In effect, each low-resolution global solution can be viewed as a new problem on which the ANM process is repeated to form a pyramid structure. This procedure, which effectively reduces the order of the problem, is called ANM with solution pyramiding, or ANM/P.

B. Background

The traditional and most computationally inefficient solution methods are those that involve complete solutions of the elemental Biot-Savart integral.[3,4] The vorticity is traced in a Lagrangian sense as material elements while it convects through the field. The method results in a nonlinear system of ordinary differential equations for the Lagrangian variables that are used as markers to follow the vorticity. These are referred to as direct or naive solution methods because they require the calculation of all of the individual point-to-point interactions in the field. The accuracy and resolution of a direct solution for the velocity field at an instant in time is limited by the $\mathcal{O}(N^2)$ cost of the calculation, where N is the number of vortex elements used in the vortex model.

A second class of solution methods,[5–7] referred to as particle-mesh methods, or vortex-in-cell methods, essentially reduce the

number of calculations by interpolating the vorticity onto a regular fixed grid, solving the vorticity transport equation on the grid, and then, finally interpolating the grid calculations onto the collocation points. The advantage of these methods lies in the use of an efficient solution procedure for the vorticity equation. Most often the computational domain must be periodic to obtain increased levels of computational efficiency. In general, many vortex problems are not periodic in any direction. A finite grid could conceivably be constructed for traditional difference schemes, but the boundary conditions would be approximate. In many engineering applications, the computational grid would have to contend with both rotating and nonrotating parts, as well as body-fitted coordinates.

A third class of computational schemes are known as grouping methods.[8–10] These schemes reduce the order of the free vortex problem by reducing the number of direct interactions which need to be computed. The basic observation common to these methods is that as the distance from a group of elements increases, their combined induced velocity approaches that of a single stronger superelement located within the group. The superelement represents an expansion of the group-induced velocities around a group centerpoint. Typically, the accuracy of the expansion depends on the number of terms used and the distance to the evaluation point. Evaluation points in the near field of a group require direct evaluation to predict the local nonlinearities correctly.

The most efficient of these techniques is the method of fast multipole expansions (FME).[11,12] This technique uses hierarchical groups consisting of an expansion in spherical harmonics of the original field to formulate a problem of $\mathcal{O}(N)$, where N is the number of elements in the field. The required accuracy determines a priori the number of terms needed in the multipole expansion and the maximum grouping depth. Initial computational overhead is required for cell generation, possibly for each time step in a highly dynamic problem, rendering the method somewhat limited for highly dynamic systems. This approach, however, produces enormous computational savings for massive quasistatic problems.

Within the framework of grouping methods, many other solution procedures have been proposed. Spalart and Leonard[9] have tried a two-dimensional approach which uses a fixed grid to define group boundaries. Subsequently, many variations have been tried to increase both the efficiency and accuracy of this type of method. The reader is urged to refer to the survey by Leonard[10] to find a more detailed discussion of other grouping methods or to the work of Anderson and Greengard[13] which offers a overview of vortex methods.

As previously discussed, the resolution of computational elements modeling a vortical flowfield is governed by the accuracy required to capture the large velocity gradients in the spatial near field, although the bulk of the element calculations are in the far field, where the high resolution of the near field is unnecessary. The ANM method[1,2,14–17] is a grouping method that involves a low resolution far-field model that is combined with a higher resolution near-field solution via a matching solution. Because of the nature of the matching, ANM has the advantage that there is no fixed grid, mesh, or computational cell involved. As such, the method can freely evolve with the flowfield, thereby simplifying the logic and accounting that is usually associated with a fixed grid structure. These advantages extend to the ANM method with pyramiding.

II. Problem Formulation

A. Analytical Numerical Matching

Analytical/numerical matching is a hybrid technique that combines analytical and numerical solutions by a matching procedure. ANM allows a global low-resolution numerical solution and a local high-resolution analytical solution to be combined formally by asymptotic matching to construct an accurate composite solution. Both the numerical and analytical solutions are simpler and more easily obtained than the solution of the original problem, and the overall solution procedure is more efficient computationally than a direct approach to the original problem. In addition, the ANM approach has the ability to provide a high degree of spatial resolution in local areas without great computational burden.

Analytical/numerical matching was developed by Bliss at Duke University. The method has been applied to several problems in vortex dynamics, aerodynamics, and acoustics. These problems include: evaluation of the Biot-Savart integral for a vortex filament[1,2]; the behavior of a vortex filament very near a surface[14,15]; vortices cut by a rotor disk[15,16]; the rollup of a two-dimensional vortex sheet; acoustic radiation and structural acoustic scattering[17]; and, most recently, to an aerodynamic panel method. In all cases, very accurate solutions were obtained with a dramatic reduction in computational cost (factors of 3–100).

ANM is somewhat similar to the method of matched asymptotic expansions (MAE),[18–20] but it differs in several important ways. The goal of ANM is to find an accurate solution to a physical problem having small scales or rapid variations that challenge the accuracy of the numerical method. In ANM, an artificial smoothing of the physical problem is introduced. The smoothing length scale must be larger than the scale associated with the numerical discretization, thereby assuring that the numerical solution of the smoothed problem is very accurate. However, the actual problem has a physical length scale smaller than the numerical discretization. The local region associated with the small scale is solved separately (usually analytically, but perhaps numerically) as a local problem that captures the small scales and rapid variations. This local problem, because of its idealizations, becomes increasingly invalid with increasing distance from the local region of rapid change.

The numerical problem and the local problem are combined by asymptotic matching. This approach requires a matching solution that is similar to the local problem but solved with the smoothing imposed. The composite solution is then given by the low-resolution global numerical solution plus the high-resolution local solution minus the matching solution, namely,

$$\begin{aligned}\text{Composite soln.} = {} & \text{low-resolution numerical soln.} \\ & + \text{high-resolution local soln.} \\ & - \text{smoothed local matching soln.}\end{aligned}$$

In the local region, the matching solution subtracts away the local error associated with the smoothed numerical solution, leaving the local solution. Far from the local region, the local solution and the matching solution cancel, since they become identical beyond the smoothed region. For the method to work well, the smoothing must be chosen to achieve an overlap so that the transition zone between the local and numerical solutions is accurate.

Referring to Fig. 1, the application of ANM to the calculation of a velocity field due to a vorticity distribution proceeds as follows. The problem to be solved is the motion of a vortex sheet, modeled for simplicity as a line of point vortices. Now consider an equivalent line of vortices with finite cores (distributed vorticity) of sufficient size that the cores overlap substantially. The sheet with fat cores is added and subtracted from the original without changing the velocity field (since the two opposite sign fat-core lines exactly cancel). Now the problem can also be viewed as the fat-core line plus the difference between the original line and the fat-core line. However, the difference between the original line and the fat-core line is purely local since their far-field contributions cancel (the far field being beyond the fat-core size, where the difference between point vortices and distributed vortices is indistinguishable). Thus, the problem can be viewed as the velocity of a line of fat-core vortices plus a local correction. The line of overlapping fat-core vortices is the low-resolution global problem to be solved numerically. The local problem consists of a few discrete vortices minus their fat-core counterparts, namely, the high-resolution local solution minus the smoothed local matching solution.

For the present work, fat-core vortices were modeled with a modified form of the Biot-Savart law,[21] Eq. (1), which artificially accounts for the effects of a rotational vortex core by including an algebraic smoothing function which removes the velocity singularity and attenuates the near-field velocity.

$$v = -\frac{\Gamma}{4\pi}\int_r \frac{\boldsymbol{r}\times \mathrm{d}\boldsymbol{s}(\gamma)}{\left[r^2+r_c^2\right]^{\frac{3}{2}}} \tag{1}$$

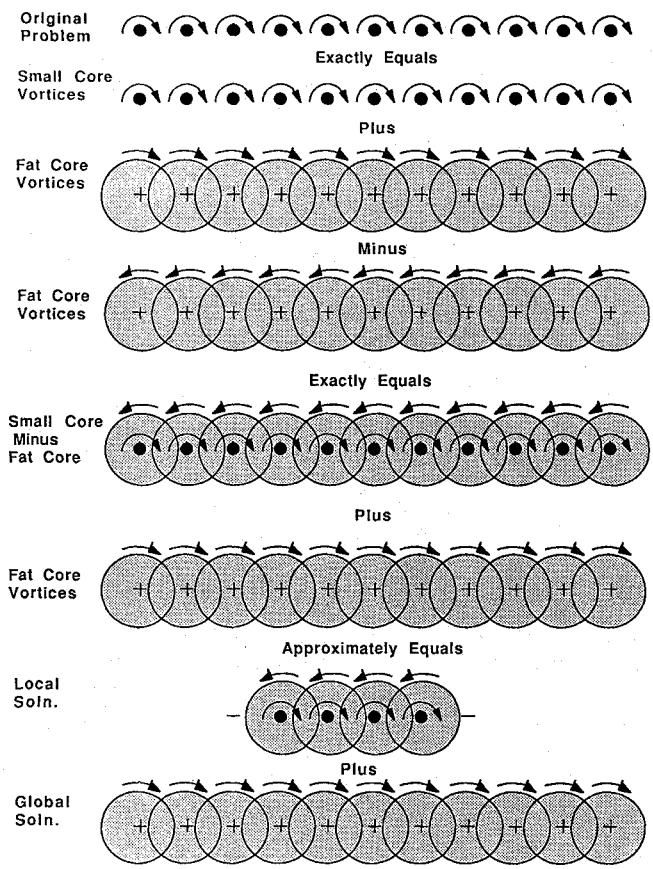

Fig. 1 Construction of the ANM solution.

The constant core radius r_c effectively spreads the vorticity across a finite area and removes the velocity singularity on the vortex itself. This particular core treatment, in addition to being functionally simple, results in an algebraic decay of the core effect with radial distance from the center of the vortex and is noted as one of the earliest core treatments described in the literature.[22] Integrating Eq. (1) along an infinite straight line results in the following expression for swirl velocity.

$$v_\theta = -\frac{\Gamma}{2\pi}\frac{r}{r^2 + r_c^2}\hat{e}_\theta \tag{2}$$

In the limit as r_c approaches zero, Eq. (2) reduces to the potential vortex result.

$$v_\theta = -\frac{\Gamma}{2\pi r}\hat{e}_\theta \tag{3}$$

Note that different core functions and length scales can be chosen and, as such, each core manifests itself differently by changing the velocity and vorticity fields accordingly.[23]

The ANM approach has several advantages. The global numerical problem is smoothed thereby avoiding the possibility of singular behavior. Furthermore, the global problem can be further approximated by a sparser distribution of fat-core vortices representing the centroids of set of vortices, as shown in Fig. 2. This approximation can be done because of the smoothed, distributed nature of the problem. It is in part from this reduction in problem size that much of the increase in computational efficiency derives since only the motion of centroids must be tracted dynamically. The velocity calculation is proportional to the square of the number of points calculated, and this number can be substantially reduced by only tracking centroids. Note that the local correction is relatively simple, and the calculation is linearly proportional to the number of vortices, not their square.

B. Solution Pyramiding

Once the ANM procedure has been applied, as just described and shown in Figs. 1 and 2, one contribution to the velocity field

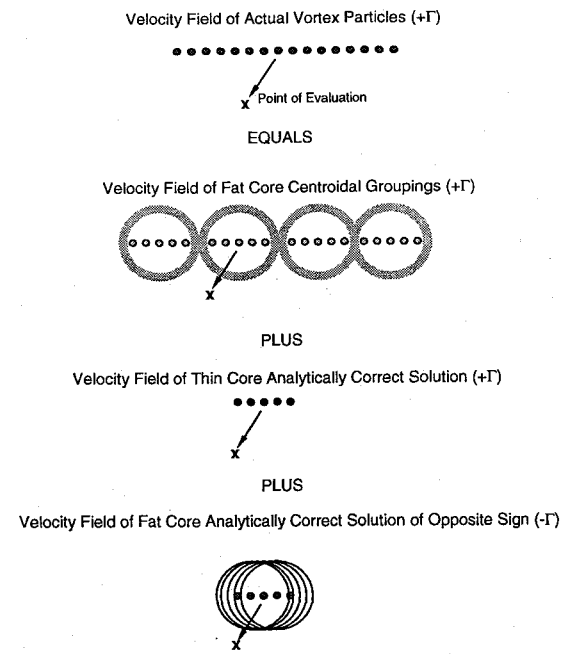

Fig. 2 ANM solution with centroidal groupings.

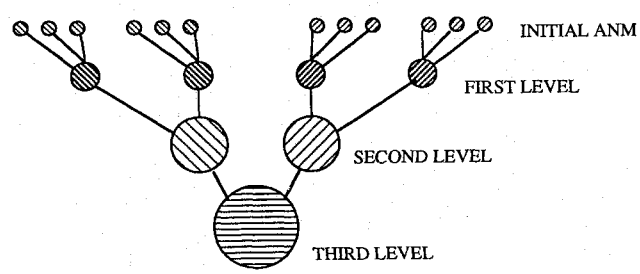

Fig. 3 Schematic representation of pyramiding.

is given by the global problem with fat-core centroidal vortices. Note, however, that this problem is of the same form as the original problem in that it is just another line of vortices, albeit sparser and with larger cores. Clearly, the ANM process can be repeated on this portion of the problem: introducing even fatter cores, breaking into local and global parts, reducing the new global problem with centroidal vortices, etc. This procedure leads to yet another global problem with an even sparser set of fatter core centroidal vortices. The process can be repeated further to form a hierarchy or pyramid of solutions, as shown schematically in Fig. 3, resulting in ANM with solution pyramiding, or ANM/P.

As shown later, this pyramiding procedure has the effect of reducing the operation count. In other words, the computation time is no longer proportional to the square of the number of vortices, but to some smaller power. The more times pyramiding is applied, the closer this power approaches unity. In practice, the gains from pyramiding are most worthwhile when the problem is large.

III. Numerical Results

A. Two-Dimensional Results

The rollup of a finite free vortex sheet, modeled here by a line of point vortices, is a suitable example for testing the two-dimensional implementation of the ANM/P methodology due to its simplicity and ease of implementation. Dynamically, the rollup behavior of the vortex sheet offers many similarities to the behavior of the vortex filaments that are commonly used in many potential-based methods used to simulate vortex wake dynamics. Specifically, constant strength vortex sheets are very familiar in the framework of inviscid aerodynamics, particularly panel methods.

Rollup of a Free Vortex Sheet

In these simulations, all of the point vortices had the same strength and were initially oriented along a straight line. The velocity fields were calculated using Eqs. (A1) and (A3), see the Appendix.

To examine the feasibility of the method, three basic test cases were investigated. The reference results that are used for comparison were found using a fully converged point vortex analysis. The relative size of a problem is dictated by the number of elements in the reference solution. For example, in a problem involving 400 computational elements, solutions are found using both the traditional Lagrangian and the ANM/P methodology and, subsequently, the results of both calculations are compared for accuracy and computer time savings.

The first test case used the basic ANM methodology without a pyramiding routine; the second case used the full ANM/P methodology with one level of pyramiding; and the third case used the full ANM/P methodology with two levels of pyramiding. In each case, all vortices were fitted with correct sign thin cores and opposite sign fat cores. In general, the thin-core magnitude was on the order of the spacing between neighboring vortices, and the fat-core magnitude was on the order of the total distance between the particles contained within each centroid. For proper matching, the local solution required a number of vortices at least equal to the number of vortices contained within a centroidal group, plus a few additional vortices to assure a smooth transition from the inner solution to the outer solution. As such, the number of vortices used in the local solution had to be large enough to fill the gap in the vorticity field created by the smoothing effect of the fat-core far-field solution thereby allowing the large near-field velocity gradients to be resolved accurately.

The implementation of ANM/P in two dimensions does not involve higher order corrections to the far-field solution; as such the far-field solution was of lowest order. It will later be demonstrated that in three dimensions the addition of the higher order correction terms to the far field can indeed further increase the accuracy of the method. Therefore, it is a reasonable expectation that the higher order corrections can increase the accuracy of the results in two dimensions as well.

Figure 4 shows examples of ANM/P calculations using different levels of pyramiding. The results of a velocity calculation for a vortex sheet of 400 rectilinear vortices is shown in Fig. 4a. The vortices were distributed along the x axis at five unit intervals. The fat-core value used was 20.0 units. The thin-core value used was 5.0 units. Each centroid encompassed four vortices. The ratio of the thin core to the particle spacing (ζ) was 1.0, and the ratio of the fat core to the centroid spacing (ζ_f) was 1.0. The vortex positions were time stepped using a fourth-order Runge–Kutta numerical integration scheme. A reference solution was computed for purposes of comparison using the traditional Lagrangian method of considering each point-to-point interaction individually. After 100 time steps, the relative spatial error in the ANM/P calculation without pyramiding was 0.35%. The maximum spatial error was found only at the tips of the vortex sheet (the first few and last few vortices of the sheet). The inner vortices were almost indistinguishable from the reference solution, with only a fraction of a percent of spatial error (on the order of 0.05%). This result is expected because the tips of the vortex sheet experience the largest induced velocities. The reader is reminded, however, that this level of accuracy is achieved with a fairly simple far-field solution comprised of vortex elements of the lowest order. As presented, without pyramiding, this case ran three times faster than the Lagrangian reference solution. These results were typical for all cases without pyramiding, and as such, considering the limited size of the field of vortex elements, a considerable gain in computational efficiency was made.

Figure 4b presents another ANM/P velocity calculation for a vortex sheet of 400 rectilinear vortices. This calculation used pyramiding. After the computational domain was divided into the first level ANM/P domain, the ANM/P methodology was applied again, effectively resubdividing the computational domain into a near field, a midfield and a far field. The vortices were distributed along the x axis at five unit intervals. The first level fat-core value used was 20.0 units and the second level fat-core value used was 50 units. The thin core used was 5.0 units, again proportional to the spacing between neighboring vortices. Each midfield centroid encompassed four vortices and each far-field centroid encompassed two midfield centroids. The ratio of the thin core to the particle

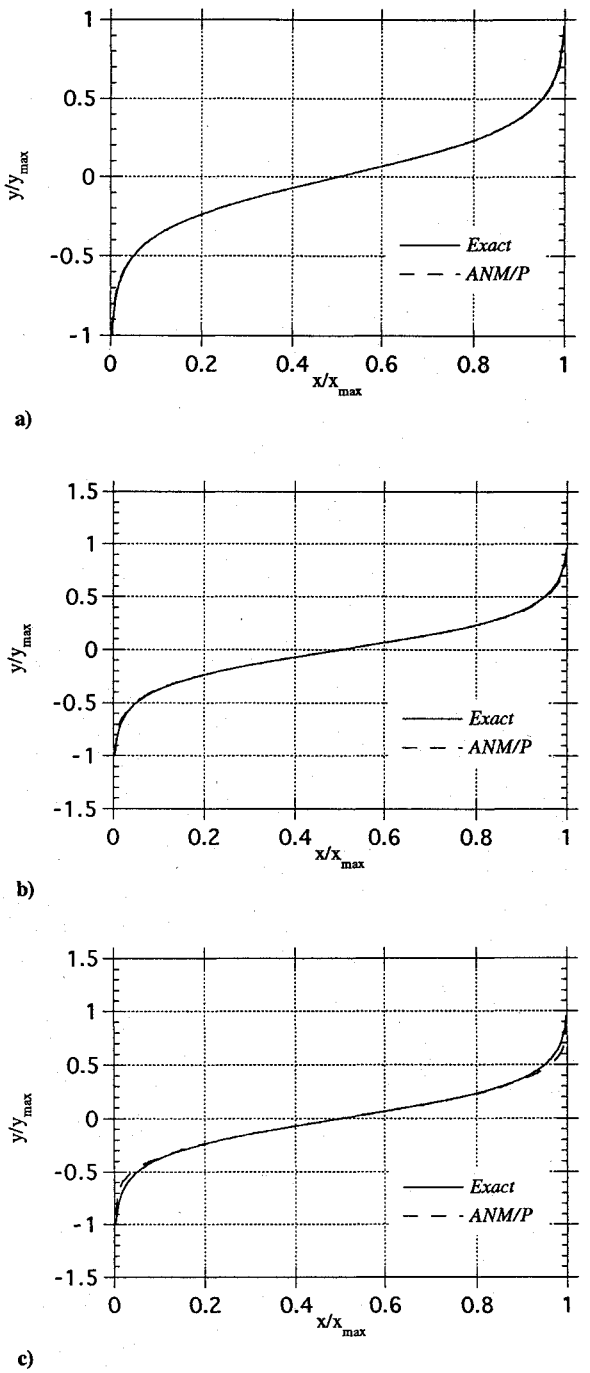

Fig. 4 Displacement of a line of point vortices calculated by ANM/P with different levels of pyramiding: a) ANM without pyramiding, b) ANM/P with one level of pyramiding, and c) ANM/P with two levels of pyramiding.

spacing (ζ) was 1.0, the ratio of the midcore to the midfield particle spacing (ζ_m) was 1.0, and the ratio of the fat core to the far-field particle spacing (ζ_f) was 1.0. Using a fourth-order Runge–Kutta numerical integration scheme, the vortex positions were time stepped. After 100 time steps, the relative spatial error in the ANM/P calculation was 0.45%. Again, the maximum spatial error was found only at the tips of the vortex sheet. The inner vortices only had a fraction of a percent of spatial error (on the order of 0.07%). Additionally, one would expect that this error could be reduced with the addition of a higher order correction term to the far-field solution. As presented, with one level of pyramiding, this case ran four and one-half times faster than the Lagrangain reference solution. Again, this represents a considerable gain in computational efficiency for a field of vortices of such limited size.

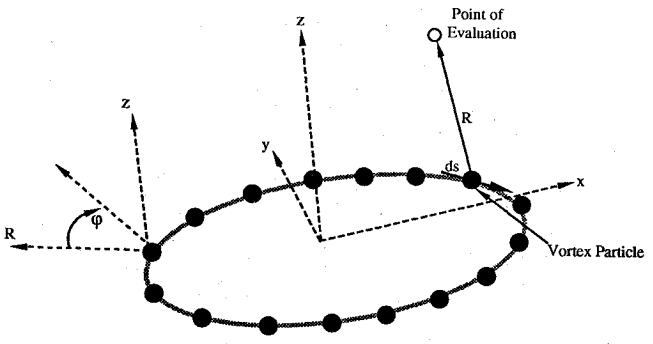

Fig. 5 Schematic representation of a ring of vortex particles.

Figure 4c shows an ANM/P velocity calculation for a vortex sheet of 400 rectilinear vortices utilizing two levels of pyramiding. Accordingly, the ANM/P methodology was applied three times to subdivide the computational domain into a near field, a submidfield, a midfield, and a far field. The vortices were distributed along the x axis at five unit intervals. The first-fat core (submidcore) value used was 20.0 units, the second fat-core (midcore) value used was 50 units, and the third fat-core value used was 80 units. The thin core used was 5.0 units. Each submidfield centroid encompassed four vortices, each midfield centroid encompassed two submidfield centroids, and each far-field centroid encompassed two midfield centroids. The ratio of the thin core to the particle spacing (ζ) was 1.0, the ratio of the submidcore to the submidfield particle spacing (ζ_{sm}) was 1.0, the ratio of the midcore to the midfield particle spacing (ζ_{sm}) was 1.0, and the ratio of the fat core to the far-field particle spacing (ζ_f) was 1.0. The vortex positions were time stepped. After 100 time steps, the relative spatial error in the ANM/P calculation was 0.55%. Again, the maximum spatial error was found only at the tips of the vortex sheet. The inner vortices had only a small percent of spatial error (on the order of 0.09%). This case ran five times faster than the Lagrangain reference solution.

These simulations show a significant gain in computational efficiency nevertheless keeping absolute errors very small. The computational savings offered by ANM/P with two levels of pyramiding over ANM/P with one level of pyramiding would be much greater if a larger problem (more vortices) were considered, as will be shown later. There is no doubt, in small problems such as these, the addition of an higher order correction to the far field would make the compromise between accuracy and efficiency less significant.

B. Three-Dimensional Results

The following discusses the results for a three-dimensional implementation of the ANM/P methodology. The problem of the velocity field induced by a single closed circular vortex filament (vortex ring) will be presented, thereby setting the foundation for ANM/P work in three dimensions. The vortex ring is a familiar and intriguing example of a flow with circular streamlines, and it exhibits dynamical behavior similar to that of many vortical flowfields of practical engineering interest. Finally, the ANM/P analysis of a multiple closed circular filament system (system of interacting rings) is presented, demonstrating the effectiveness of the method on far larger systems that entail a more detailed structure.

Velocity Field of a Vortex Ring

The vortex ring was modeled with vortex particles or vortons, namely, elemental discretizations of the Biot-Savart law, see Eq. (A6) in the Appendix. Figure 5 shows a schematic representation of a vortex particle ring. In Fig. 5, a global coordinate system is placed at the center of the ring, and a local cylindrical coordinate system is centered on each vortex particle. The ring collocation points were equally spaced around the azimuth. The reference solutions used for comparison were found using a fully converged Lagrangain vortex particle analysis, which considers each point-to-point interaction. In the reference solutions, the overlap of the thin core values were chosen such that the numerical solution obtained would no longer vary with the addition of more vortex particles, therefore, the vortex particle solution represents the converged solution for a discrete vortex ring with a finite core radius. The relative size of a problem is dictated by the number of elements in the reference solution. For example, in a problem involving 1000 computational elements, solutions are found using both the traditional Lagrangian and the ANM/P methodology and, subsequently, the results of both calculations are compared for accuracy and computer time savings.

One level of pyramiding was used in the vortex ring calculation. Centroidal groups were calculated azimuthally along the circumference of the ring. The velocity was calculated on the ring collocation points. The vortex particle positions were used as collocation points. The ring was modeled with 1000 vortex particles, the ring radius was 100 units, the fat-core value was 10.0 units, the midcore value was 1.75 units, and the thin-core value was 0.63 units. The near-field domain had 20 particles in it, the midfield domain had 20 particles in it, and the far-field domain had 50 particles in it. The ratio of the ring radius to the fat core ($\lambda = R_{\text{ring}}/t_c$) was 10.0. The ratio of the thin core to the particle spacing (ζ) was 1.3, the ratio of the midcore to the midfield particle spacing (ζ_m) was 1.3, and the ratio of the fat core to the far-field particle spacing (ζ_f) was 1.3. The computational time for the ANM/P solution was over one order of magnitude (11.1 times) faster than the Lagrangain reference solution.

The binormal velocity field was calculated along radial paths normal to the ring spanning different azimuthal locations, and velocity field calculations were made along binormal paths intersecting the ring at different azimuthal locations. Figure 6a shows the binormal velocity induced along radial stations. The ANM/P predicted velocity is practically indistinguishable from the Lagrangian velocity prediction. Figure 6b shows the binormal velocity component predicted along a binormal path intersecting the ring at one azimuthal station. Again the ANM/P predicted velocity and the Lagrangain reference solution are almost indistinguishable. The maximum error occurs just off the ring and falls off within about two fat-core radii. Figure 6c shows the normal velocity component in different horizontal planes parallel to the plane of the ring predicted along the previous binormal path tangent to the ring at an azimuthal station. Again, the ANM/P predicted velocity is practically indistinguishable from the Lagrangain reference solution.

The velocities calculated using the ANM/P method were slightly less than the similar Lagrangain reference solution. This characteristic reduction in the ANM/P velocity is due to the smoothing effect of the fat core, a similar effect was seen in the two-dimensional vortex sheet case. The relative error in the velocity field was 1.3% along a radial path of integration with the maximum error on or near the vortex ring itself. The maximum occurs within the neighborhood of the ring because a vortex particle can not identically induce velocity on itself, it can only be affected by the other particles in the spatial field that surround it. The level of accuracy is quite remarkable considering the simplicity of the model. The far field was modeled with vortex elements of the lowest order, which required no higher order correction. So far, the method presents itself as an efficient way to calculate velocity, within the frame work of a rather simple model.

All of the calculations were repeated with a higher order correction added to the far-field model. All of the parameters were held the same except for the number of particles used in the midfield solution. This was reduced due to the increased accuracy of the elements used, with the hope of increasing even further the efficiency of the solution. Only 18 particles were used in the midfield solution. The higher order correction used was derived from the next term in the Taylor series expansion of the velocity field induced by the group of vortex elements about its centroid, and again represents the addition of a very simple algebraic expression to the far-field equations. In all cases, as expected, the velocity calculations were almost indistinguishable from the Lagrangain reference solution. The ANM/P solution with the one higher order correction was 11.5 times faster than the reference solution, but the relative error was only 0.7% along a radial path of integration, again with the maximum error on or near the vortex ring itself. For the sake of simplicity, no other higher order corrections were added to the solution. Because the

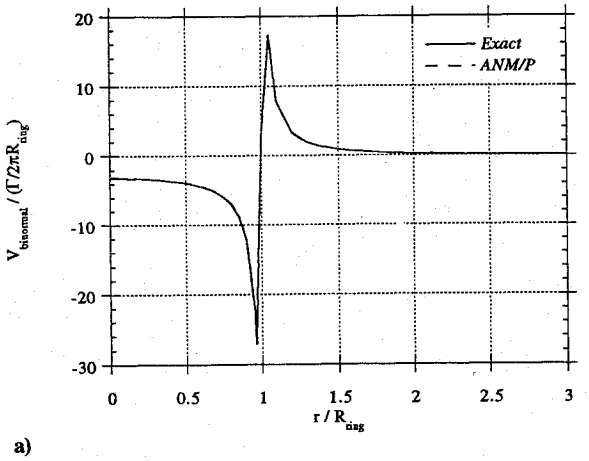

a)

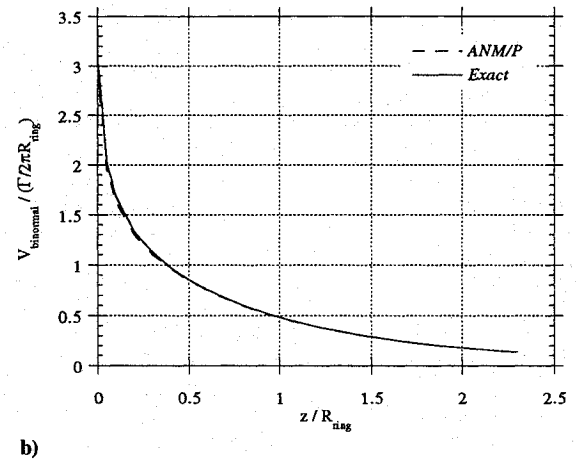

b)

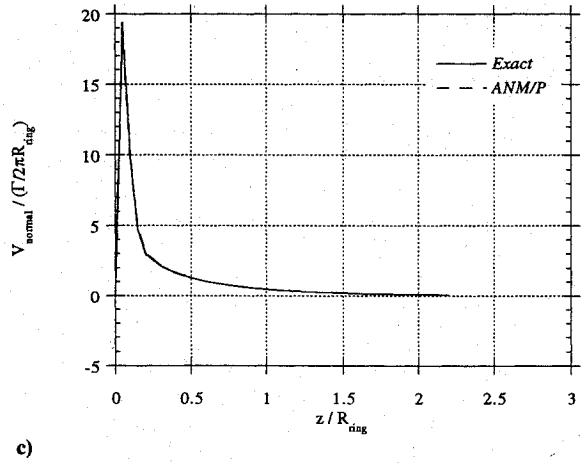

c)

Fig. 6 ANM/P velocity calculation for a ring of vortex particles with one level of pyramiding; a) binormal velocity along radial stations, b) binormal velocity along a binormal path, and c) normal velocity along binormal tangent to ring.

method is fully expandable to much higher order, one would expect that the relative error would decrease with the addition of more correction terms. Again, the ANM/P method accurately and efficiently calculates vortex velocities within the framework of a simple and practical methodology.

Velocity Field of a System of Interacting Vortex Rings

The multiple ring problem is interesting because the vortical system exhibits two distinct forms of dynamical behavior. In the near field, the system of rings is highly dynamic and the rings rotate about one another. In the far field, a smooth binormal propagation velocity is globally self-induced, and the entire system translates with uniform speed.

The velocities induced by multiple concentric vortex rings of different radii located in vertically parallel planes were calculated. Geometrically, this system is like an aggregate vortex ring made of constituent vortex ring filaments. The initial distance between each individual vortex ring was chosen such that it was much less than the radius of curvature of the global ring, thus assuring that each ring was at least within one thin-core radius of every other ring. This case tested the three-dimensional ANM/P methodology with one level of pyramiding.

In the single ring case, it was shown that the addition of an higher order correction to the far-field and midfield centroidal grouping make the ANM/P calculations more accurate. In other words, the compromise between accuracy and efficiency becomes less significant. For the sake of brevity, the following calculations only use centroidal solutions of the lowest order, however, these centroidal solutions are easily generalized to higher-order by the addition of other terms. Therefore, by using high-order centroidal groups, a higher level of accuracy is expected.

Vortex quasi-three-dimensional centroids were calculated at cross-sectional stations along different azimuthal positions of the global ring. This three-dimensional centroid model uses the symmetry of the interacting rings and their large radius of curvature to locally collapse a three-dimensional computational domain into a two-dimensional domain. In the near field of any point on a ring, due to the large radius of curvature of the interacting ring system, the point in question can only see the approximately straight portion of the neighboring rings in the near field. As such, the neighboring rings can be considered locally as infinite straight filaments, and the centroid can be calculated, at least locally, in the usual two-dimensional sense. This quasi-three-dimensional model has been substantiated by numerical experiment for systems with large radius of curvature.

Pyramid groups were calculated azimuthally along the ring circumference. All of the cases presented used one level of pyramiding.

The first case presented consists of a system of three vortex rings. Each vortex ring is comprised of 100 vortons (Biot-Savart discretizations). The rings have equivalent radii and are oriented concentricity in different horizontal planes. The near-field domain was modeled with 20 points on each ring, the midfield domain was modeled with 20 points on each ring and the far-field domain was modeled with 25 points. The thin core was 2.25 units, the midcore was 4.95 units, and the fat core was 9.75 units. The ratio of the ring radius to the fat core ($\lambda = R_{\text{ring}}/f_c$) was 10.25. The ratio of the thin core to the particle spacing (ζ_t) was 1.5, the ratio of the midcore to the midfield particle spacing (ζ_m) was 1.5, and the ratio of the fat core to the far-field particle spacing (ζ_f) was 1.5. The computational time for the ANM/P solution was 4.5 times faster than the Lagrangian reference solution.

The following results were calculated on the first ring. This is the ring that lays in the horizontal plane below the other two rings. Calculating the velocity components on a ring provides a rigorous test of the methodology, because the maximum error occurs within the neighborhood of the over-lapping thin cores, and the second ring is located in this region. Again, this error is partially due to the lack of a vortex particle self-induced velocity. Similar to the single ring case, outside this region the error drops off rapidly. Actually, outside this region the two calculations are practically indistinguishable.

The z component of the induced velocity is constant about the azimuth. The ANM/P calculated velocity was slightly less than the reference calculation, again this was due to the fat-core numerical smoothing and the self-induced velocity deficit. There was a 2.7% relative error in the z component. Figure 7 shows the x and y velocity components. Both of the ANM/P predicted velocities are almost indistinguishable from the reference solutions. The y component had 0.95% relative error, whereas the x component had 0.92% relative error.

The second case is a vortex system consisting of three vortex rings, but each vortex ring consists of 1000 vortex particles. The vortex rings are oriented concentrically with equivalent radii in different horizontal planes. The near-field domain was modeled with 10 vortons on each ring, the midfield domain was modeled with 20

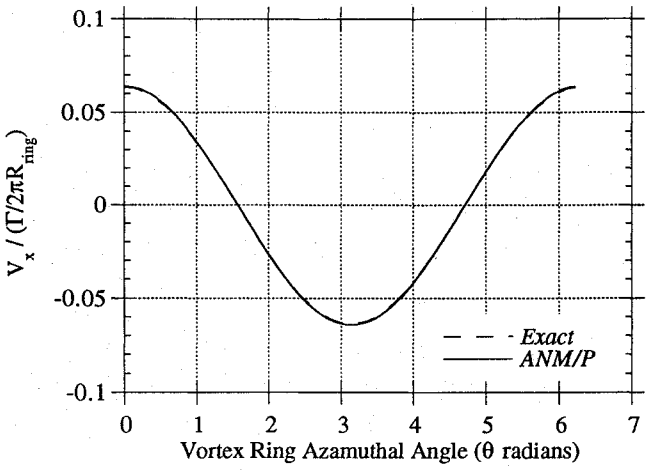

a)

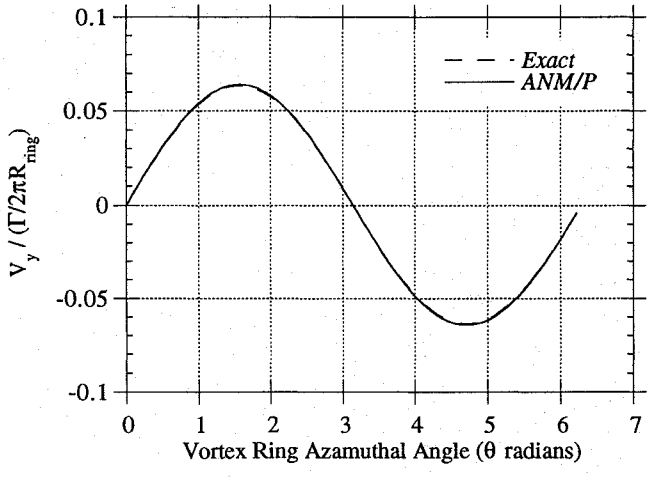

b)

Fig. 7 Velocity components for a ring of vortex particles in a multiple ring system, calculated using ANM/P with one level of pyramiding; a) x component of velocity induced on ring 1 and b) y component of velocity induced on ring 1.

vortons on each ring, and the far-field domain was modeled with 25 vortons. The thin core was 0.63 units, the midcore was 1.75 units, and the fat core was 10.00 units. The ratio of the ring radius to the fat core ($\lambda = R_{\text{ring}}/t_c$) was 10.00. The ratio of the thin core to the particle spacing (ζ_t) was 1.3, the ratio of the midcore to the midfield particle spacing (ζ_m) was 1.3, and the ratio of the fat core to the far-field particle spacing (ζ_f) was 1.3. The computational time for the ANM/P solution was over an order of magnitude faster (21.1 times) faster than the Lagrangain reference solution. Numerical experiments demonstrated that orienting the rings concentrically with different sized radii in the same plane offers similar results.

Again, the following results were calculated on the first ring. The ANM/P predicted velocity is slightly less than the reference solution due the error factors previously discussed. There was 2.0% relative error in the x component. Upon close inspection, there are small fluctuations in the ANM/P predicted velocity field, which are due to slight irregularities in the far-field and mid-field solutions. The irregularities are manifestations of nonsmooth centroidal overlap regions. The irregularities can be washed out if more vortex particles are used in the near-field solution, but this in turn increases the computational cost. In the y component there was a 1.9% relative error, and in the z component there was a maximum of 5% relative error. Again, due the fat-core smoothing, the ANM/P predicted velocity is slightly less than the reference prediction. The relative percent error in the z component is the greatest because the velocities in the z direction tend to be very small when compared to other parts of the velocity field, therefore, small errors become magnified when they are normalized by small reference values. Therefore, for a better feeling of the magnitude of the error, the relative error can be normalized by a characteristic velocity of the field, for example, by $\Gamma/2\pi t_c$. In that case, there is only 0.024% relative error.

The preceding calculations were done to the lowest order. No higher order correction was used to modify the centroidal groupings. As discussed earlier, greater accuracy can be expected if higher order corrections are used, however, considering the simplicity of the lowest order model, the levels of accuracy achieved are remarkable.

Although the computational savings offered by ANM/P with one level of pyramiding was significant, it is expected that for larger systems two or three levels of pyramiding will offer even more dramatic computational savings. For this system, there was a reduction of over 20 times the Lagrangain reference solution. Again, this savings is remarkable considering the simplicity of the model and the ease of implementation.

IV. Issues of Practical Accuracy and Efficiency

Applying the ANM/P method to a particular problem requires the definition of several parameters; such as the various core radii (t_c, m_c, f_c), the size of the domain of local computational elements used at different levels of the computational pyramid (M_l, N_l) and the ratio of the core magnitude to the particle spacing (ζ core magnitude/element spacing). Each of these parameters will affect the resulting velocity prediction. This section discusses basic issues that are relevant to these decisions.

The parameters ζ_t, ζ_m, and ζ_f represent the ratio of the two length scales involved in an ANM/P analysis. The parameters are defined as $\zeta_t = t_c/\{\text{average near-field element spacing}\}$, $\zeta_m = m_c/\{\text{average midfield element spacing}\}$, and $\zeta_f = f_c/\{\text{average far-field element spacing}\}$. This parameter controls the numerical smoothing of the low-resolution outer solution. If this parameter is too large, the outer solution exhibits overly smooth behavior, and the ANM/P velocity predictions will be lower than actual values. On the other hand, if this parameter is too small, the outer solution is not smooth and will have cyclic variations in its spatial vorticity distribution resulting in cyclic variations in the magnitude of the ANM/P velocity prediction. Variable core size centroidal groupings were investigated. The ratio of the ANM/P velocity to the Lagrangain velocity was calculated as a function of the ratio of the core radius to the centroid spacing. The most accurate solutions, those that offered a good inner-outer solution match, occurred when the core radius was on the order of the spacing between the centroids. If the core size is smaller than the spacing between the far-field centroids, the solution match falls off. This fall off occurs because the solution is not represented by a smooth vorticity field, and there are vorticity gaps in the field. On the other hand, if the core size is much larger than the particle spacing the far-field solution becomes overly smooth, and the solution match falls off again due to over smoothing. From numerical experimentation, the size of the ratio used should be $0.5 < \{\zeta_t, \zeta_m, \zeta_f\} < 1.5$, in both two and three dimensions.

The number of elements in the midfield domain M_L and the local domain N_L significantly affect the strong flowfield gradients. If they are chosen too large, an effective point of diminishing returns is met and the flowfield is modeled accurately but not efficiently. If M_L and N_L are chosen too small, the large gradients in the flowfield are not modeled accurately in the numerical model, and an oversimplified (smooth) velocity field is predicted. If chosen correctly, an effective model of the flowfield is obtained at a greatly reduced numerical cost. A numerical study showed that in both two and three dimensions the local domain of particles should be at least large enough to fill the fat-core radii at the common level of the computational pyramid. In other words, if the thin core t_c magnitude is 10 units and the local particle spacing is 1 unit, then at least 10 local particles are needed to fill the fat core at that level of the computational pyramid.

V. Analytical/Numerical Matcing with Pyramiding Optimum Operation Count

The explicit two-dimensional result for plain ANM (no levels of pyramiding) and ANM/P with one level of pyramiding will be analytically derived, then the generalized extension to three dimensions with an infinite number of pyramid levels will be derived following mathematical induction.

Consider a two-dimensional vortex sheet of length L consisting of N rectilinear vortices. Let α and β be overlap constants defined by

$$\beta = \frac{1}{\zeta} = \frac{\text{vortex spacing}}{\text{fat-core radius}} \tag{4}$$

$$\alpha = \frac{N_L}{N_{L_{\min}}} = \frac{\text{size of local domain used}}{\text{minimum size of local domain}} \tag{5}$$

where N_L is the local computational domain size, $N_{L_{\min}}$ is the minimum local computational domain size (without overlap), and ζ is the ratio of the fat core radius to the element spacing. Additionally, define N_C as the number of far-field centroids, R_f as the fat-core radius, R_t as the thin-core radius, and C_0 as the ANM pyramiding constant (the subscript is equal to the number of pyramid levels). The ANM dispersion constant is defined by κ,

$$\kappa = \alpha/\beta \tag{6}$$

From the physical geometry and computational aspects of the vortex sheet problem, the following equation for the total number of operations can be derived:

$$O_{\text{count}} = N \cdot N_L + N \cdot N_C \tag{7}$$

In Eq. (5.4), the first term on the right-hand side represents the number of calculations done in the near field. Each Nth computational element is multiplied by the number of elements in the local computational domain. The second term on the right-hand side represents the contribution of the far-field domain, each Nth computational element is multiplied by the number of far-field centroidal groupings.

Using the geometry of the problem, the following relations for N_L and N_C are derived:

$$N_L = N(\alpha R_f/L) \tag{8}$$

$$N_C = L/\beta R_f \tag{9}$$

Substituting these relations in Eq. (7) leads to an expression for the operation count,

$$O_{\text{count}} = N\left(N\frac{\alpha R_f}{L}\right) + \left(N\frac{L}{\beta R_f}\right) \tag{10}$$

To find a relative maximum or minimum, the partial derivative of Eq. (10) with respect to R_f is found and set equal to zero,

$$\frac{\partial O_{\text{count}}}{\partial R_f} = \frac{N^2\alpha}{L} - \frac{NL}{\beta R_f^2} = 0 \tag{11}$$

Solving the homogeneous algebraic Eq. (11) for an optimum value of R_{f_m} leads to

$$R_{f_m} = L(1/\alpha\beta N)^{\frac{1}{2}} \tag{12}$$

Back substituting Eq. (12) into Eqs. (8) and (9) leads to the following optimum values for N_L and N_C:

$$N_L = (N\alpha/\beta)^{\frac{1}{2}} \tag{13}$$

$$N_C = (N\alpha/\beta)^{\frac{1}{2}} \tag{14}$$

Now substituting Eqs. (13) and (14) into Eq. (7) gives the following relation for the optimum order count:

$$O_{\text{count}} = C_0 N^{\frac{3}{2}} \tag{15}$$

where C_0 is given by

$$C_0 = 2(\kappa)^{\frac{1}{2}} \tag{16}$$

Considering a similar analysis with the addition of one level of pyramiding, Eqs. (7) and (10) become

$$O_{\text{count}} = N \cdot N_L + N \cdot N_{C2} + N \cdot N_C \tag{17}$$

$$O_{\text{count}} = N\left(N\frac{\alpha R_f}{L}\right) + N\left(N_{C2}\frac{\alpha R_{f2}}{L}\right) + \left(N\frac{L}{\beta R_f}\right) \tag{18}$$

respectively, where N_{C2} is the number of midfield centroids, and R_{f2} is the midcore radius. The middle term in Eqs. (17) and (18) represents the contribution of the midfield domain. Each Nth computational element is multiplied by the number of elements in the midfield computational domain.

Again, taking the partial derivatives with respect to $\{R_f, R_{f2}\}$ and setting the result equal to zero gives the following system of coupled nonlinear algebraic equations:

$$\left\{\begin{aligned} \frac{\partial O_{\text{count}}}{\partial R_f} &= \frac{N}{L} - \frac{R_{f2}}{\beta R_f^2} = 0 \\ \frac{\partial O_{\text{count}}}{\partial R_{f2}} &= \frac{\alpha}{R_f} - \frac{L}{R_{f2}^2} = 0 \end{aligned}\right\} \tag{19}$$

As before, solving this homogeneous system leads to the optimum values for $\{R_f, R_{f2}\}$, which in turn leads to optimum values for $\{N_L, N_C, N_{C2}\}$. Substituting the values for $\{N_L, N_C, N_{C2}\}$ in to Eq. (17) gives an optimum order count of the form

$$O_{\text{count}} = C_1 N^{\frac{4}{3}} \tag{20}$$

where C_1 is given by

$$C_1 = 3(\kappa)^{\frac{2}{3}} \tag{21}$$

Continuing the same analysis for two levels of pyramiding leads to an optimum order count of the form

$$O_{\text{count}} = C_2 N^{\frac{5}{4}} \tag{22}$$

where C_2 is given by

$$C_2 = 4(\kappa)^{\frac{3}{4}} \tag{23}$$

From mathematical induction of the previous cases, the general case leads to an order count of the form

$$O_{\text{count}} = C_P N^{(3+P)/(2+P)} \tag{24}$$

where C_P is given by

$$C_P = (2+P)(\kappa)^{(1+P)/(2+P)} \tag{25}$$

The preceding analysis remains true in three dimensions, because both the two-dimensional and three-dimensional analysis deal with a field of discrete particles, where the addition of a spatial dimension does not effect the operation count or total number of computational elements used.

For example, consider a two-dimensional vortex sheet modeled with 400 rectilinear vortices using the plain ANM scheme. The model parameters are $\zeta = 1.5$, $P = 0$, $N_L = 14$, $N_{L_{\min}} = 8$, and $N = 400$. Following the analysis just outlined, the required parameters are found to be $\beta = 0.666$, $\alpha = 1.75$, and $\kappa = 2.625$. Substituting the preceding parameters into Eq. (15) and normalizing by N^2 demonstrates that an optimum ANM/P implementation for this model should offer a savings of six times over the traditional method. A computer run of the previous case offered a time savings of about four times over the traditional result. This result is not surprising, because the previous analysis does not take into account computer overhead costs and the work thus far with ANM/P has been focused on developing the methodology, not optimizing it. However, the previous results show that once fully developed and optimized, the ANM/P methodology should offer substantial savings in computational effort over the traditional vortex methods.

VI. Discussion of Analysis

Aside from the intrinsic interest the present problem possesses, it is of considerable value as an accelerated vortex method for aerodynamic applications. ANM/P, even without higher order corrections, offers levels of accuracy necessary for application in vortex-based panel methods and wake models. Preliminary research has demonstrated that a vortex- and doublet-based panel method implemented with ANM/P is a viable means for the aerodynamic calculation.

Strictly speaking, it should be pointed out that the ANM/P vortex method as discussed in this paper is not an ad hoc method but rather has rigorous mathematical roots. The lowest order centroidal solution can be thought of as an expansion of the global solution with the higher order terms removed. However, without a loss of generality, these terms can be added to the centroidal expression to offer a global solution higher order accuracy. It must be pointed out that the lowest order solution provides a level of accuracy that is satisfactory for many aerodynamic applications. The local solutions can also be refined for added accuracy. The two solutions are put together via the local matching solution. Similar to the perturbation method of matched asymptotic expansions, the outer limit of the local solution must be equal to the inner limit of the low-resolution outer solution. In this manner, the composite solution is formed.

The ANM/P methodology is general. The technique, matching a high-resolution local solution to a low-resolution global solution, has been applied to a multitude of fluid dynamic problems including applications in acoustics, rotor aerodynamics, and aerodynamic panel methods.

VII. Conclusions

The present work has described an accelerated vortex method. The major conclusions are as follows

1) An accelerated vortex method has been developed without a loss of mathematical rigor. The method is well suited for dynamic problems, because no fixed grid structure is necessary. The approach naturally distinguishes between near-field and far-field effects.

2) Numerical results have been obtained for vortex sheet rollup, for vortex ring motion, and for interacting vortex rings. All results illustrate high accuracy and large gains in computational efficiency, as high as a factor of 20 in the present work. Accuracy can be further improved with higher order corrections, with a minimal effect on computational efficiency.

3) Additional work, both analytical and numerical, is needed to explore the other possible applications for the analytical/numerical matching methodology.

Appendix: Extension of the Vortex Centroid Approximation to Higher Order

If we consider the velocity induced by a group (or subgroup) of n equal strength two-dimensional point vortices, the Biot-Savart integral (in vector notation) in two dimensions reduces to

$$V = \frac{\Gamma}{2\pi} \sum_{i=1}^{n} \frac{\boldsymbol{k} \times \boldsymbol{r}_i}{|\boldsymbol{r}_i|^2} \tag{A1}$$

where $\boldsymbol{k}$ is the normal unit vector out of the plane of the flow, parallel to the vortex lines; and $\boldsymbol{r}_i$ is the vector between the ith point vortex the point of evaluation. Now define $\boldsymbol{r}_i = \boldsymbol{R} + \Delta\boldsymbol{r}_i$, where the vector $\boldsymbol{R}$ goes from the centroid of vorticity[24] to the point of evaluation and the vector $\Delta\boldsymbol{r}_i$ goes from the ith vortex to the centroid. In two dimensions the centroid of vorticity is analogous to the concept of the mass center from the theory of dynamic systems.

After substitution and manipulation to group terms in the parameter $\Delta r_i/R$, this parameter is assumed small, and the expression is expanded in a Taylor series. As a result of the definition of the centroid, the linear terms in the expansion are identically zero. Neglecting all of the terms of order $(\Delta r_i/R)^3$ and greater, the result can be written as

$$V = \frac{\Gamma}{2\pi R} \times \left[\left[\left(\boldsymbol{k} \times \frac{\boldsymbol{R}}{R} \right) \left(n - \frac{1}{R} \sum_{i=1}^{n} nD^2 + \frac{4}{R^4} \sum_{i=1}^{n} (\boldsymbol{R} \cdot \Delta\boldsymbol{r}_i)^2 \right) \right] - \frac{2}{R^3} \sum_{i=1}^{n} [(\boldsymbol{k} \times \Delta\boldsymbol{r}_i)(\boldsymbol{R} \cdot \Delta\boldsymbol{r}_i)) \right] \tag{A2}$$

where $R = |\boldsymbol{R}|$, and $D = \Delta\vec{r}_i \cdot \Delta\vec{r}_i$ represents the dispersion of vorticity[21] about the centroid. This expansion becomes inaccurate and fails as the point of evaluation approaches the centroid, namely, as $R \to 0$.

The first term in the series given by Eq. (A2) is the velocity induced by a single-point vortex of strength $n\Gamma$ placed at the position of the vortex centroid. This term is the first approximation to the velocity field induced by the entire group of individual vortices. Although this term alone can be quite accurate in approximating the velocity field of the entire group of vortices, it carries no shape information about the vortex groupings. Groupings of a complicated nature may not be modeled accurately at points nearer the grouping. The additional higher order terms carry the missing shape information that is necessary for a more accurate representation of the velocity field.

For point vortices with distributed cores, the general formula for the velocity is

$$V = \frac{\Gamma}{2\pi} \sum_{i=1}^{n} \frac{\boldsymbol{k} \times \boldsymbol{r}_i}{|\boldsymbol{r}_i|^2 + r_c^2} \tag{A3}$$

where r_c is a vorticity smoothing length scale. Following the development of Eq. (A2), a similar expansion can be derived for a grouping of vortices with smooth cores. However, it is now advantageous to expand in the small parameter $\Delta\vec{r}_i/\sqrt{R^2 + r_c^2}$, which is never singular and can be kept small even as $R \to 0$ by the appropriate choice of r_c. The resulting expansion is

$$V = \frac{\Gamma}{2\pi} \frac{1}{R^2 + r_c^2} \left[\left\{ (\boldsymbol{k} \times \boldsymbol{R}) \left[n - \left(\frac{1}{R^2 + r_c^2} \right) \sum_{i=1}^{n} nD^2 + \frac{4}{\left(R^2 + r_c^2\right)^2} \sum_{i=1}^{n} (\boldsymbol{R} \cdot \Delta\boldsymbol{r}_i)^2 \right] \right\} - \frac{2}{\left(R^2 + r_c^2\right)} \sum_{i=1}^{n} [(\boldsymbol{k} \times \Delta\boldsymbol{r}_i)(\boldsymbol{R} \cdot \Delta\boldsymbol{r}_i)] \right] \tag{A4}$$

The same comments apply to Eq. (A4) as applied to Eq. (A2). Both expressions represent the velocity field induced by a vortex placed at the centroid of vorticity with additional correction terms to account for the shape of the grouping. There is no restriction on the location of the point vortices in the field. However, because the expansion parameter cannot become large, Eq. (A4) does not exhibit singular behavior anywhere in the field. Furthermore, numerical studies show the expansion remains quite accurate for values of the expansion parameter of order one. Therefore, Eq. (A4) can be used in both the spatial near and far fields of the vortex grouping, and provides a fairly simple higher order correction for shape information in a distributed vorticity field. Note that the existence of such a correction for smeared vortices and the absence of singular behavior is one of the advantages of the overall method.

As an illustration of Eq. (A4), the specific result is cited for a continuous line of smeared (fat-core) point vortices of length $2l$.

The derivation involves integrating a distribution of the smoothed singularities, with total circulation Γ and core r_c, from $-l$ to l about

the origin. The approximate velocity in cylindrical polar coordinates is given by

$$u(r,\theta) = -\frac{\Gamma}{2\pi r}\left[\left(\frac{r^2\sin\theta}{r^2+r_c^2}\right) - \left(\frac{l}{r}\right)^2\left(\frac{\frac{1}{3} - \left[\cos^2\theta/\left(\sin^2\theta + (r_c/r)^2\right)\right]}{\left\{1+\left[\cos^2\theta/\left(\sin^2\theta+(r_c/r)^2\right)\right]\right\}^3}\right)\left\{\frac{\sin^2\theta}{\left[\sin^2\theta+(r_c/r)^2\right]^2}\right\}\right]$$

$$v(r,\theta) = \frac{\Gamma}{2\pi r}\left[\left(\frac{r^2\cos\theta}{r^2+r_c^2}\right) + \left(\frac{l}{r}\right)^2\left(\left[\frac{\cos\theta}{1+(r_c/r)^2}\right]^3 - \left\{\frac{\cos\theta}{\left[1(r_c/r)^2\right]^2}\right\}\right)\right] \tag{A5}$$

Again note that the first term in the expansion is the expression for the vortex centroid. Therefore, the preceding result can be interpreted, similar to the earlier analysis, as the centroid term with additional higher order corrections. This form was used for the higher order corrections in the two-dimensional simulations used in this paper.

Although the preceding discussion offers higher order corrections for two dimensions, the extension to three dimensions is not entirely straightforward because there is no general analytical expression for a three-dimensional centroid for vorticity. Instead, the three-dimensional extension for higher order correction is based on the a short segment of a vortex filament. This approach is analogous to the difference, in two dimensions, between a point vortex and a linear distribution, as discussed earlier.

A direct discretization of the Biot-Savart integral into a Riemann sum gives the three-dimensional velocity field as the sum of vortex particles, or vortons. The formula shown next includes the effect of smearing using the core length scale r_c.

$$V = \frac{\Gamma}{4\pi}\sum_{i=1}^{n}\frac{\boldsymbol{r}_{v_i}\times\boldsymbol{l}_{s_i}}{\left[r_{v_i}^2+r_c^2\right]^{\frac{3}{2}}} \tag{A6}$$

Note that Eq. (A6) becomes the expression for the discretized Biot-Savart integral without smearing when $r_c \to 0$. To extend this representation to higher accuracy, the expression for the velocity field of a smoothed, straight vortex filament of length l is given next in local cylindrical polar coordinates,

$$V = \frac{\Gamma}{4\pi r} \times \left\{\frac{x+\frac{1}{2}l}{\sqrt{\left(x+\frac{1}{2}l\right)^2+r^2+r_c^2}} - \frac{x-\frac{1}{2}l}{\sqrt{\left(x-\frac{1}{2}l\right)^2+r^2+r_c^2}}\right\}\hat{e}_\theta \tag{A7}$$

where the filament is centered on the x axis. In the spirit of the previous analysis, Eq. (A7) can be expanded in a Taylor series in the expansion parameter

$$\varepsilon = \frac{\left(\frac{1}{2}l\right)}{\sqrt{x^2+r^2+r_c^2}} \tag{A8}$$

Neglecting terms of order (ε^5), the result is

$$V = \frac{\Gamma}{4\pi r}\left\{\frac{lr^2}{\left(x^2+r^2+r_c^2\right)^{\frac{3}{2}}} + \left(\frac{l}{2}\right)^3\frac{4x^2-r^2-r_c^2}{\left(x^2+r^2+r_c^2\right)^{\frac{7}{2}}}\right\}\hat{e}_\theta \tag{A9}$$

The first term in Eq. (A9) is simply a vorton, or more precisely, one piece of the discretized form of the Biot-Savart integral. The second term contains shape information, accounting for the degree of extension of the filament. Because of the choice of expansion parameter, Eq. (A9) is never singular, and numerical studies show it can provide good accuracy throughout the flowfield for reasonable choices of ε. This analysis demonstrates that a short segment of vortex filament can be modeled as a simple vorton plus a simple higher order correction. This form was used for the vortex ring simulations with higher order corrections.

References

[1]Bliss, D. B., and Miller, W. O., "Efficient Free Wake Calculations Using Analytical/Numerical Matching and Far-Field Linearization," Proceedings of the 45th Annual Forum of the American Helicopter Society, Boston, MA, May 1989.

[2]Bliss, D. B., and Miller, W. O., "Vortex Filament Calculations by Analytical/Numerical Matching with Comparison to Other Element Methods," AIAA 9th Computational Fluid Dynamics Conf., Buffalo, NY, June 14–16, 1989.

[3]Rosenhead, L., "The Formation of Vortices From a Surface Discontinuity," *Proceedings of the Royal Society of London*, Ser. A, Vol. 134, 1931, p. 170.

[4]Bliss, D. B., Teske, M. E., and Quackenbush, T. R., "A New Methodology for Free Wake Analysis Using Curved Vortex Elements," NASA CR 3958, Dec. 1987.

[5]Baker, G. R., "The 'Cloud in Cell' Technique Applied to the Roll Up of Vortex Sheets," *Journal of Computational Physics*, Vol. 31, 1979, pp. 76–95.

[6]Christiansen, J. P., "Numerical Simulation of Hydrodynamics by the Method of Point Vortices," *Journal of Computational Physics*, Vol. 13, 1973, pp. 363.

[7]Couët, B., Buneman, O., and Marshall, F. J., "Simulation of Three-dimensional Incompressible Flows with a Vortex-in-Cell Method," *Journal of Computational Physics*, Vol. 39, 1980, p. 305.

[8]Anderson, C., "A Method of Local Corrections for Computing the Velocity Field Due to a Distribution of Vortex Blobs," *Journal of Computational Physics*, Vol. 62, 1985, p. 111.

[9]Spalart, P. R., and Leonard, A., "Computation of Separated Flows by a Vortex-Tracing Algorithm," *AIAA Journal*, Vol. 81, 1981, p. 1246.

[10]Leonard, A., "Vortex Methods For Flow Simulation," *Journal of Computational Physics*, Vol. 37, 1980, pp. 289–335.

[11]Greengard, L., and Rokhlin, V., "A Fast Algorithm for Particle Simulation," *Journal of Computational Physics*, Vol. 73, 1987, p. 325.

[12]Greengard, L., *The Rapid Evaluation of Potential Fields in Particle Systems*, MIT Press, Cambridge, MA, 1988.

[13]Anderson, C., and Greengard, C., "On Vortex Methods," *SIAM Journal of Numerical Analysis*, Vol. 22, 1985, p. 413.

[14]Quackenbush, T. R., and Bliss, D. B., "Free Wake Calculation of Rotor Flow Fields for Interactional Aerodynamics," *Vertica*, Vol. 14, No. 3, 1990, pp. 313–327.

[15]Quackenbush, T. R., and Bliss, D. B., "Free Wake Calculation of Rotor Flow Fields for Interactional Aerodynamics," Proceedings of the 44th Annual Forum of the American Helicopter Society, Washington, DC, June 1988.

[16]Quackenbush, T. R., Bliss, D. B., and Mahajan, A. J., "High Resolution Flow Field Prediction for Tail Rotor Aeroacoustics," *Proceedings of the 45th Annual Forum of the American Helicopter Society*, Boston, MA, May 1989.

[17]Bliss, D. B., and Peretti, L. P., "Prediction of Acoustic Radiation Using Analytical/Numerical Matching," 124th Meeting of the Acoustical Society of America, New Orleans, LA, Oct. 1992.

[18]Van Dyke, M., *Perturbation Methods in Fluid Mechanics*, Parabolic Press, Stanford, CA, 1975.

[19]Ashley, H., and Landahl, M., *Aerodynamics of Wings and Bodies*, Dover, Mineola, NY, 1965.

[20]Bender, C. M., and Orszag, S. A., *Advanced Mathematical Methods for Scientists and Engineers*, McGraw-Hill, New York, 1978.

[21]Bliss, D. B., and Miller, W. O., "Efficient Free Wake Calculations Using Analytical/Numerical Matching," *Journal of the American Helicopter Society*, Vol. 38, No. 2 , 1993, pp. 43–52.

[22]Rosenhead, L., "The Spread of Vorticity in the Wake Behind a Cylinder," *Proceedings of the Royal Society of London*, Ser. A, Vol. 127, 1930, pp. 590–612.

[23]Ting, L., and Klein, R., "Viscous Vortical Flows," *Lecture Notes in Physics*, Vol. 374, Springer-Verlag, NY, 1991.

[24]Batchlor, G. K., *An Introduction To Fluid Mechanics*, Cambridge Univ. Press, Cambridge, England, UK, 1967.